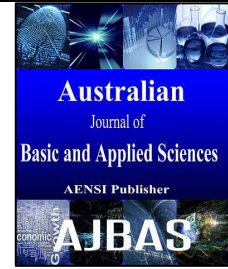




ISSN:1991-8178

## Australian Journal of Basic and Applied Sciences

Journal home page: www.ajbasweb.com



### Efficiency Improvement InZVS DC-DC Converter Using Snubber

<sup>1</sup>E.Parameswari and <sup>2</sup>P.Karagavalli<sup>1</sup>PG scholar, Department of Electrical and Electronics Engineering, Government College of Engineering, Salem-11, Tamil Nadu, India.Salem-11, Tamil Nadu, India.<sup>2</sup>Assistant Professor, Department of Electrical and Electronics Engineering, Government College of Engineering,

#### ARTICLE INFO

##### Article history:

Article Received 12 January 2015

Revised 1 May 2015

Accepted 8 May 2015

##### Keywords:

Bidirectional dc-dc converter, lossless active snubber, zero-voltage-switching.

#### ABSTRACT

An efficiency improvement in ZVS switched dc-dc converter using snubber is proposed in this project. In this proposed converter, zero voltage switching (ZVS) of main switches is achieved by utilizing an active snubber which consists of auxiliary switches, diodes, an inductor and a capacitor. Although conduction losses associated with additional components increase, switching losses are significantly reduced due to the ZVS operation of main switches. Therefore, total efficiency is improved. Moreover, there is no reverse-recovery problem of the intrinsic body diodes of the switches. The total amount of the current flowing through the auxiliary circuit decreases significantly since the active snubber operates during the short time intervals. Therefore, conduction losses in main switches and auxiliary circuit are significantly reduced and thus overall efficiency is improved. Moreover, by utilizing the snubber circuit, there is no reverse-recovery phenomenon that is induced by the poor dynamic performance of the MOSFETs body diode. The proposed converters are provided in order to verify ZVS and efficiency improved.

© 2015 AENSI Publisher All rights reserved.

**To Cite This Article:** E.Parameswari and P.Karagavalli., Efficiency Improvement InZVS DC-DC Converter Using Snubber. *Aust. J. Basic & Appl. Sci.*, 9(21): 149-159, 2015

#### INTRODUCTION

IN recent years, alternative energy systems and applications like eco-friendly cars have been focused on due to the exhaustion of fossil fuel and severe environmental pollution. Bidirectional dc-dc converters are one of the most important energy conversion system in the applications such as plug-in hybrid electric vehicle (PHEV), fuel-cell vehicle, renewable energy system, and uninterruptible power supply (UPS) (Hagbin, S., *et al.*, 2013; Cao, J. and A. Emadi, 2012; Park, T. and T. Kim, 2013; Jang, M., *et al.*, 2013; Li, W., *et al.*, 2011; Rolak, M. and M. Malinowski, 2011; Jayasinghe, S.D.G., *et al.*, 2011; Arias, M., *et al.*, 2012). In PHEV system, the bidirectional dc-dc converter acts as an energy transfer system from a low voltage battery to a DC-link that is an input voltage of an inverter for operating a vehicle motor, or from a DC-link to a battery for charging regenerative energy (Hagbin, S., *et al.*, 2013; Cao, J. and A. Emadi, 2012). In the renewable energy systems, including fuel cell systems, photovoltaic systems, and wind power systems, the bidirectional dc-dc converter is essential for electric power conversion between a low voltage battery where dump power is charged and a high voltage source for home appliances (Park, T. and T.

Kim, 2013; Jang, M., *et al.*, 2013; Li, W., *et al.*, 2011; Rolak, M. and M. Malinowski, 2011; Jayasinghe, S.D.G., *et al.*, 2011). The bidirectional dc-dc converter is divided into an isolated type and a non-isolated type (Yao, C., *et al.*, 2011; Lee, J.-Y., *et al.*, 2011; Vinnikov, D. and I. Roasto, 2011; Wu, T.-F., *et al.*, 2010; Singh, R.K. and S. Mishra, 2013; Wu, H., *et al.*, 2012; Das, P., *et al.*, 2010; Das, P., *et al.*, 2009; Do, H.-L., 2011; Jung, D.-Y., *et al.*, 2013). Because an isolated bidirectional dc-dc converter has more than four switches and an isolated transformer, it has higher conduction losses and lower efficiency than a non-isolated bidirectional dc-dc converter (Yao, C., *et al.*, 2011; Lee, J.-Y., *et al.*, 2011; Vinnikov, D. and I. Roasto, 2011; Wu, T.-F., *et al.*, 2010). On the other hand, the non-isolated bidirectional dc-dc converter has high efficiency due to a simple structure (Singh, R.K. and S. Mishra, 2013; Wu, H., *et al.*, 2012; Das, P., *et al.*, 2010; Das, P., *et al.*, 2009; Do, H.-L., 2011; Jung, D.-Y., *et al.*, 2013). Recently, soft-switching techniques are applied to the non-isolated bidirectional dc-dc converter to achieve soft-switching of power switches in a wide range of load and reduce switching noises (Das, P., *et al.*, 2010; Das, P., *et al.*, 2009; Do, H.-L., 2011; Jung, D.-Y., *et al.*, 2013). Soft-switching technique makes it possible to have

**Corresponding Author:** E.Parameswari, PG scholar, Department of Electrical and Electronics Engineering, Government College of Engineering, Salem-11, Tamil Nadu, India.Salem-11, Tamil Nadu, India.  
E-mail: parameesweety@gmail.com

high efficiency by reducing switching losses, and it is necessary for miniaturization and light weight (Jung, D.-Y., *et al.*, 2013; Lin, B.-R. and C.-H.Chao, 2013). An active snubber was proposed in (Das, P., *et al.*, 2010), where analysis of the buck converter was given. Soft-switching operation of the main switch is achieved by utilizing an auxiliary circuit consisting of an additional switch, an additional diode, a resonant capacitor, and a resonant inductor. The ZVS of the main switch is achieved. However, the auxiliary circuit makes the output current ripple large. In addition, the energy stored in the resonant inductor during the reverse-recovery of the auxiliary diode can cause large voltage ringing across the switch and diode in the snubber circuit. In order to suppress the voltage ringing, additional passive snubbers are required, and it will degrade system performance. Two active snubbers were proposed in (Rolak, M. and M. Malinowski, 2011), where analysis for the boost converter was given. One of them is equal to that in (Das, P., *et al.*, 2010). Therefore, they have the same drawbacks. In order to solve these problems, a new snubber was proposed. The voltage ringing is confined to the output voltage. However, many components are required, and it will degrade system efficiency and raise the overall cost. To reduce the switching losses, digital frequency

modulation technique is also presented in (Do, H.-L., 2011; Jung, D.-Y., *et al.*, 2013). The disadvantage of this technique is that the inductor current is not continuous, and the inductor ripple current is severely large at full load. Fig.1 shows a well-known soft-switching bidirectional dc-dc converter that achieves ZVS of switches by simply adding an auxiliary inductor and a capacitor. Disadvantage of this converter is that large circulating current always flows through an auxiliary inductor and a capacitor for satisfying soft-switching of switches, irrespective of load. So, high conduction losses are induced from resistance of an auxiliary inductor, a capacitor, a printed circuit board (PCB), and switches. To overcome this problem, a soft-switching bidirectional dc-dc converter using a lossless active snubber is proposed as shown in Fig. 2. Compared with the converter in Fig. 1, the total amount of the current flowing through the auxiliary circuit decreases significantly since the active snubber operates during the short time intervals. Therefore, conduction losses in main switches and auxiliary circuit are significantly reduced and thus overall efficiency is improved. Moreover, by utilizing the snubber circuit, there is no reverse-recovery phenomenon that is induced by the poor dynamic performance of the MOSFETs' body diode.

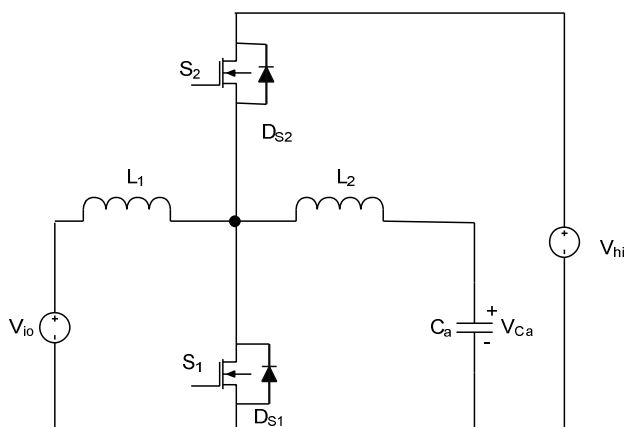


Fig. s1: Conventional soft-switching bidirectional dc-dc converter.

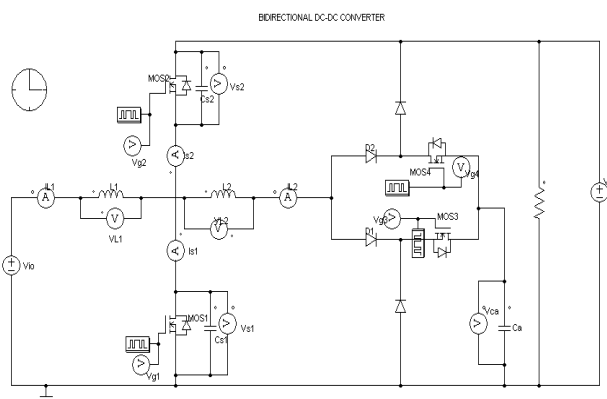
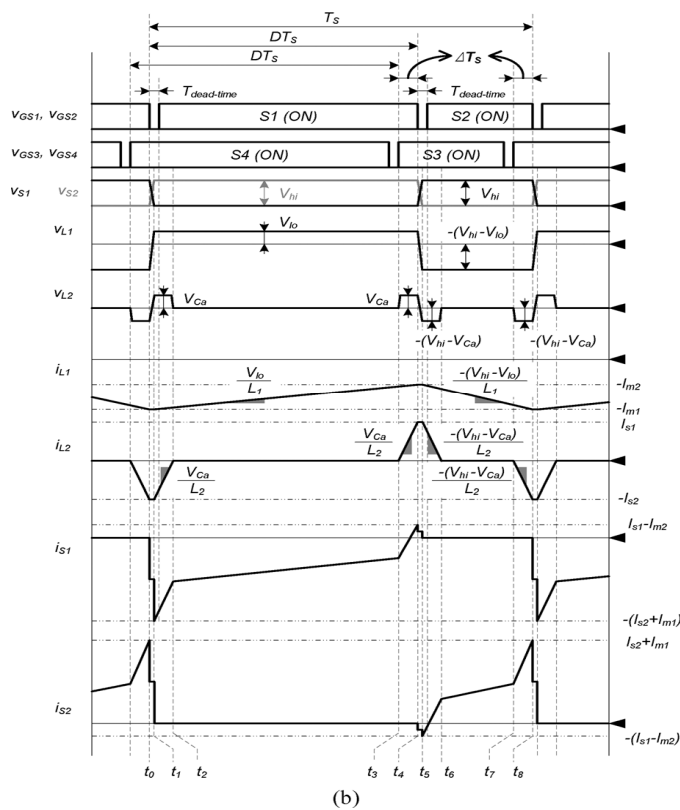
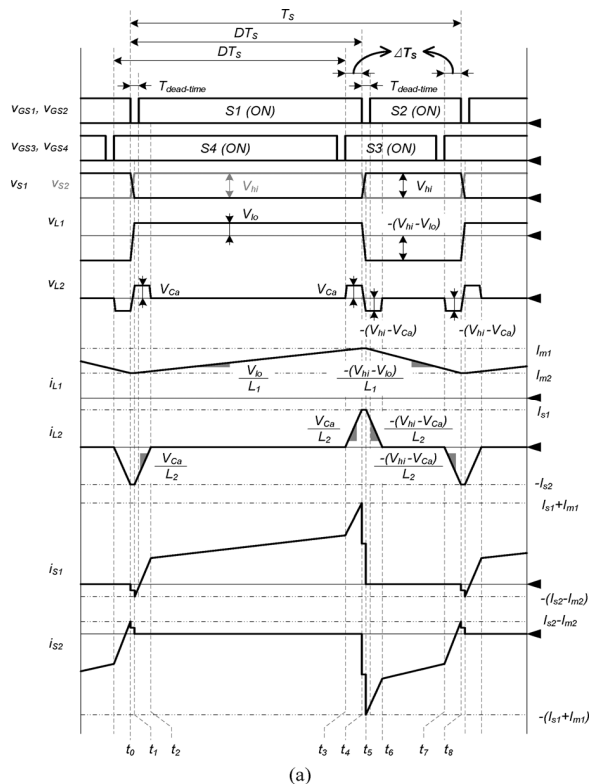


Fig. 2: Proposed bidirectional dc-dc converter.

**II. Analysis of The Proposed Converter:**

$S_1$  acts as a boost

The circuit diagram of the proposed bi-directional converter is shown in Fig. 2. The switch



**Fig. 3:** Theoretical waveforms of the proposed converter. (a) Boost operation.(b) Buck operation.

Switch to boost operation and a synchronous switch in buck operation. The switch  $S_2$  acts as a synchronous switch in boost operation and as a buck switch in buck operation. The lossless active snubber, which consists of an auxiliary inductor  $L_2$ , an additional capacitor  $C_a$ , blocking diodes  $D_1$  and  $D_2$ , and auxiliary switches  $S_3$  and  $S_4$ , is added into the conventional bidirectional dc-dc converter. In order to minimize the conduction loss in the active snubber and provide soft-switching operation of the main switches  $S_1$  and  $S_2$ , the lossless active snubber operates during short time intervals. The diodes  $D_{S1}, D_{S2}, D_{S3}$ , and  $D_{S4}$  are the intrinsic body diodes of  $S_1, S_2, S_3$ , and  $S_4$ . The diodes  $D_3$  and  $D_4$  are clamping diodes to clamp the voltages across the auxiliary switches and the blocking diodes in the snubber circuit. The capacitors  $C_{S1}$  and  $C_{S2}$  represent the parasitic output capacitances of  $S_1$  and  $S_2$ . Assuming that the capacitance of  $C_a$  is large enough,  $C_a$  can be considered as a voltage source  $V_{Ca}$  during a switching period.

The theoretical waveforms of the proposed converter in boost and buck operations are shown in Fig. 3(a) and (b), respectively. The boost and buck operations are described in Fig. 4(a) and (b). Each operation can be divided into eight modes during one switching period  $T_s$ .

### III. Operation Principle:

#### A. Boost Operation:

Before  $t_0$ , the switches  $S_2$  and  $S_4$  are conducting. The inductor currents  $i_{L1}$  and  $i_{L2}$  decrease linearly and reach their minimum values  $I_{m2}$  and  $-I_{S2}$  respectively at  $t_0$ . Since the current  $I_{S2}$  is larger than  $I_{m2}$ , the switch current  $I_{S2}$  changes the current flow direction from negative to positive as shown in Fig. 3(a).

Mode 1 [ $t_0, t_1$ ]:

The switch  $S_2$  is turned off at  $t_0$ . The parasitic output capacitor  $C_{S1}$  starts to discharge and  $C_{S2}$  begins to charge. Assuming that the parasitic output capacitor  $C_{S1}$  and  $C_{S2}$  have very small capacitor and time interval in this mode is very short, the inductor currents  $i_{L1}$  and  $i_{L2}$  can be regarded as constant and the voltages  $V_{S1}$  and  $V_{S2}$  vary linearly.

The transition time interval  $T_{t1}$  can be expressed as follows

$$T_{t1} = \frac{(C_{S1} + C_{S2})V_{hi}}{I_{S2} - I_{m2}} \quad (1)$$

Mode 2 [ $t_1, t_2$ ]:

At  $t_1$ , the voltage  $V_{S2}$  arrives at  $V_{hi}$  and  $V_{S1}$  reaches zero with the turn-on of  $D_{S1}$ . Since the switch voltage  $V_{S1}$  is zero before the gate pulse of  $S_1$  is applied, the ZVS of  $S_1$  is achieved. Since the voltages  $v_{L1}$  and  $v_{L2}$  across the each inductor are  $V_{I0}$  and  $V_{Ca}$  respectively, the inductor currents  $i_{L1}$  and  $i_{L2}$  increase linearly as follow

$$i_{L1}(t) = I_{m2} + \frac{V_{I0}}{L_1}(t - t_1) \quad (2)$$

$$i_{L2}(t) = -I_{S2} + \frac{V_{I0}}{L_2}(t - t_1) \quad (3)$$

The switch current  $i_{S1}$  is expressed as the sum of  $i_{L1}$  from (2) and  $i_{L2}$  from (3).

Mode 3 [ $t_2, t_3$ ]:

This mode begins when the inductor current  $i_{L2}$  becomes zero and the blocking diode  $D_2$  is turned off. After that, the auxiliary switch  $S_4$  is turned off in the zero-current switching (ZCS) condition. The switch current  $i_{S1}$  is equal to the main inductor current  $i_{L1}$  from (2).

Mode 4 [ $t_3, t_4$ ]:

At  $t_3$ , the auxiliary switch  $S_3$  is turned on. Since the voltage  $v_{L2}$  across the inductor  $L_2$  is  $v_{Ca}$ , the inductor current  $i_{L2}$  increases linearly with a slope of  $V_{Ca}/L_2$  as follows

$$i_{L2}(t) = \frac{V_{Ca}}{L_2}(t - t_3) \quad (4)$$

The switch current  $i_{S1}$  is the sum of  $i_{L1}$  and  $i_{L2}$  obtained from (2) and (4). At the end of this mode, the inductor currents  $i_{L1}$  and  $i_{L2}$  arrive at their maximum values  $i_{m1}$  and  $i_{S1}$ , respectively. The currents  $I_{m1}$  and  $i_{S1}$  can be obtained by

$$I_{m1} = I_{m2} + \frac{V_{I0}}{L_1}DT_s \quad (5)$$

$$i_{S1} = \frac{V_{Ca}}{L_2}\Delta T_s \quad (6)$$

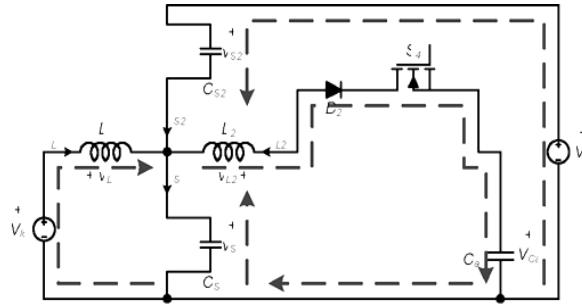
Where the duty cycle  $D$  is the ratio of the time interval,

During which the auxiliary inductor  $L_2$  is storing energy, to one switching period.

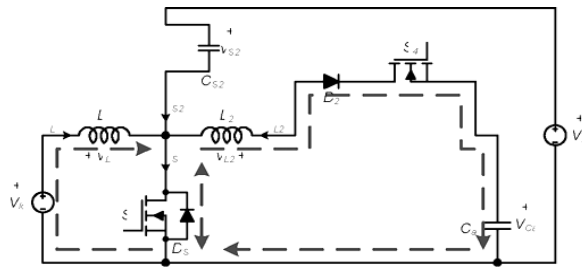
Mode 5 [ $t_4, t_5$ ]:

The switch  $S_1$  is turned off at  $t_4$ . The parasitic output capacitor  $C_{S1}$  starts to charge and  $C_{S2}$  begins to discharge. Assuming that the parasitic output capacitors  $C_{S1}$  and  $C_{S2}$  have very small capacitance and the time interval in this mode is very short, the inductor currents  $i_{L1}$  and  $i_{L2}$  can be regarded as constant and the voltages  $v_{S1}$  and  $v_{S2}$  vary linearly. The transition time interval  $T_{t2}$  can be expressed as follows

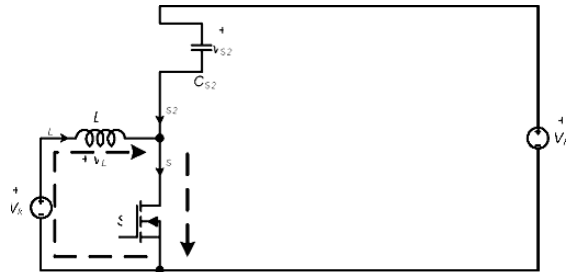
$$T_{t2} = \frac{(C_{S1} + C_{S2})V_{hi}}{I_{m1} + I_{S1}} \quad (7)$$



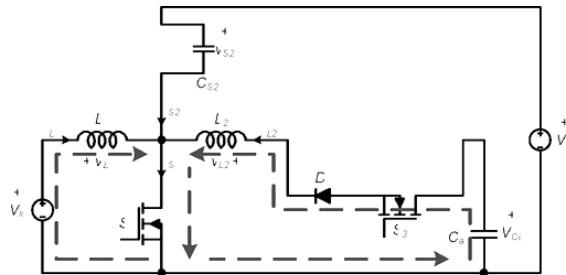
Mode1



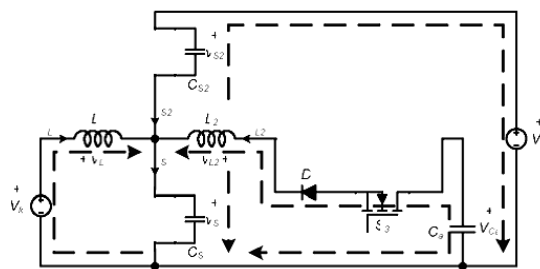
Mode 2



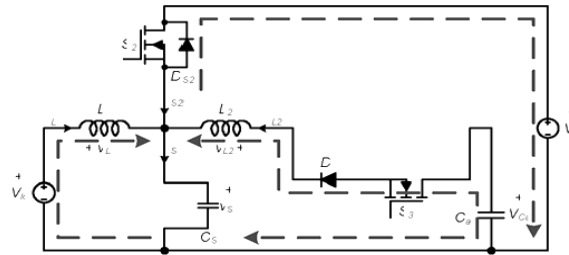
Mode3



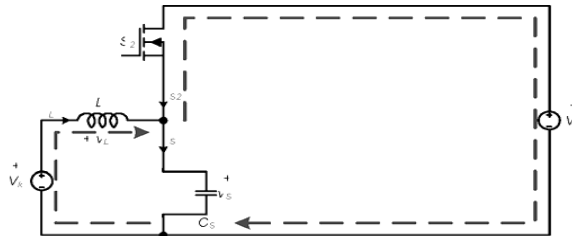
Mode4



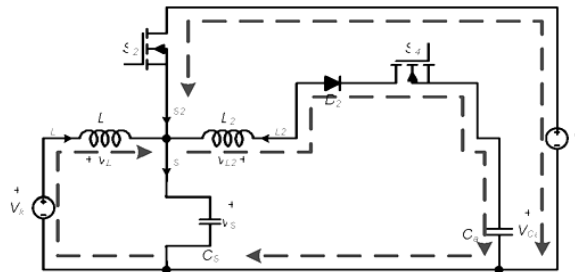
Mode5



Mode6



Mode7



Mode8

Fig. 4(a): Boost operation of the converter

Mode 6[ $t_5, t_6$ ]:

At  $t_5$ , the voltage  $v_{s1}$  arrives at  $V_{hi}$  and  $v_{s2}$  reaches zero with the turn-on of  $D_{s2}$ . Since the switch voltage  $v_{s2}$  is zero before the gate pulse of  $S_2$  is applied, the ZVS of  $S_2$  is achieved. Since the voltages  $v_{L1}$  and  $v_{L2}$  across the each inductor are  $-(V_{hi} - V_{Io})$  and  $-(V_{hi} - V_{Ca})$  respectively, the inductor currents and decrease linearly as follows:

$$i_{L1}(t) = I_{m1} - \frac{(V_{hi}-V_{Io})}{L_1}(t - t_5) \tag{8}$$

$$i_{L2}(t) = I_{s1} - \frac{(V_{hi}-V_{Io})}{L_2}(t - t_5) \tag{9}$$

The switch current  $i_{s2}$  is expressed as the sum of  $-i_{L1}$  from (8) and  $-i_{L2}$  from (9).

Mode 7[ $t_6, t_7$ ]:

This mode begins when  $i_{L2}$  zero becomes and the blocking diode  $D_1$  is turned off. After that, the auxiliary switch  $S_3$  is turned off in the ZCS condition. The switch current  $I_{s2}$  is equal to the main inductor current  $-i_{L1}$  from (8).

Mode 8[ $t_7, t_8$ ]:

At  $t_7$ , the auxiliary switch  $S_4$  is turned on. Since the voltage  $v_{L2}$  across the inductor  $L_2$  is  $-(V_{hi} - V_{Ca})$ , the inductor current  $i_{L2}$  decreases linearly with a slope of  $-(V_{hi} - V_{Ca})/L_2$  as follows

$$i_{L2}(t) = -\frac{(V_{hi}-V_{Ca})}{L_2}(t - t_7) \tag{10}$$

The switch current  $i_{s2}$  is the sum of  $-i_{L1}$  and  $-i_{L2}$  obtained from (8) and (10). At the end of this mode, the inductor currents  $i_{L1}$  and  $i_{L2}$  arrive at their minimum values  $I_{m1}$  and  $-I_{s2}$  respectively. The currents and can be obtained by

$$I_{m2} = I_{m1} - \frac{V_{hi}-V_{Io}}{L_1}(1 - D)T_S \tag{11}$$

$$-I_{s2} = -\frac{V_{hi}-V_{Ca}}{L_2}\Delta T_S \tag{12}$$

**B.Buck Operation:**

The buck operation of the proposed converter as shown in Figure.3(b) and 4(b) is similar to the boost operation except that the main inductor current  $i_{L1}$  and the switch currents  $i_{s1}, i_{s2}$  have the opposite direction of those in boost operation. Before  $t_0$ , the switches  $S_2$  and  $S_4$  are conducting. At  $t_0$ , the inductor current  $i_{L1}$  and  $i_{L2}$  are decreasing linearly and reach their minimum values  $-i_{m1}$  and  $-i_{s2}$ , respectively.

Mode 1[ $t_0, t_1$ ]:

The switch  $S_2$  is turned off at  $t_0$ . In a similar way to mode 1 in boost operation, the switch voltages  $v_{s1}$  and  $v_{s2}$  vary linearly. The transition time interval  $T_{t1}$  can be expressed as follows

$$T_{t1} = \frac{(C_{s1}+C_{s2})V_{hi}}{I_{m1}+I_{s2}} \tag{13}$$

Mode 2[ $t_1, t_2$ ]:

At  $t_1$ , the voltage  $v_{S2}$  arrives at  $V_{hi}$  and  $v_{S1}$  reaches zero with the turn-on of  $D_{S1}$ . In a similar way to mode 2 in boost operation, the ZVS of  $S_1$  is achieved. Since the voltages  $v_{L1}$  and  $v_{L2}$  across the each inductor are  $v_{Io}$  and  $v_{Ca}$  respectively, the inductor currents  $i_{L1}$  and  $i_{L2}$  increase linearly as follows

$$i_{L1}(t) = -I_{m1} + \frac{V_{Io}}{L_1}(t - t_1) \tag{14}$$

$$i_{L2}(t) = -I_{S2} + \frac{V_{Ca}}{L_2}(t - t_1) \tag{15}$$

The switch current  $i_{S1}$  is expressed as the sum of  $i_{L1}$  from (14) and  $i_{L2}$  from (15)

Mode3[[ $t_2, t_3$ ]:

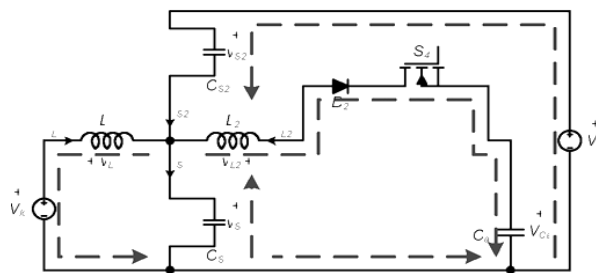
This mode begins when  $i_{L2}$  zero becomes and the blocking diode  $D_2$  is turned off. After that, the auxiliary switch  $S_4$  is turned off in the ZCS condition. The switch current  $i_{S1}$  is equal to the main inductor current  $i_{L1}$  from (14).

Mode 4[ $t_3, t_4$ ]:

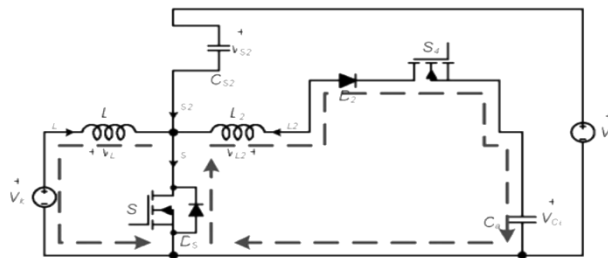
At  $t_3$ , the auxiliary switch  $S_3$  is turned on. Since the voltage  $v_{L2}$  across the inductor  $L_2$  is  $V_{Ca}$ , the inductor current  $i_{L2}$  increases linearly as follows

$$i_{L2}(t) = \frac{V_{Ca}}{L_2}(t - t_3) \tag{16}$$

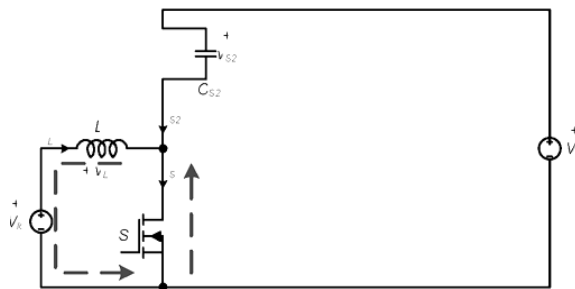
The switch current  $i_{S1}$  is the sum of  $i_{L1}$  and  $i_{L2}$  obtained from (14) and (16).



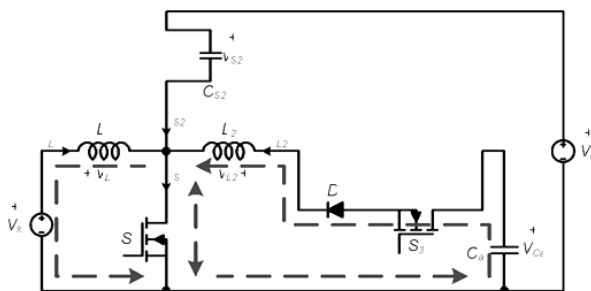
Mode1



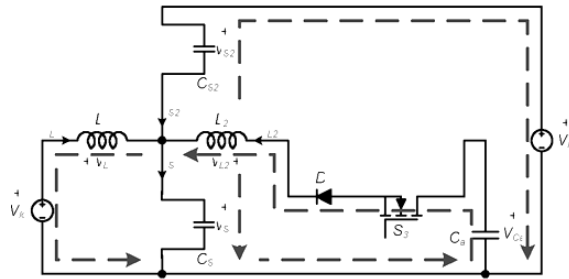
Mode2



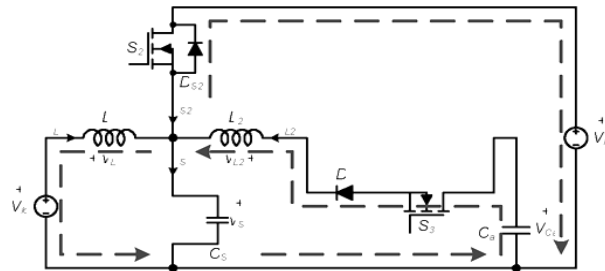
Mode3



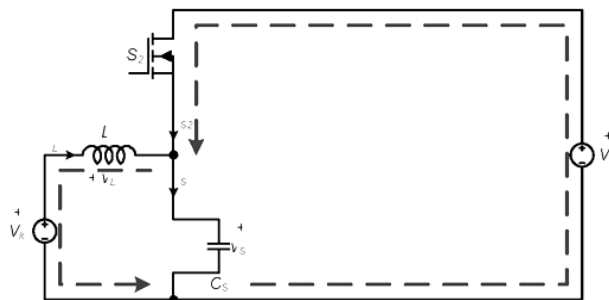
Mode4



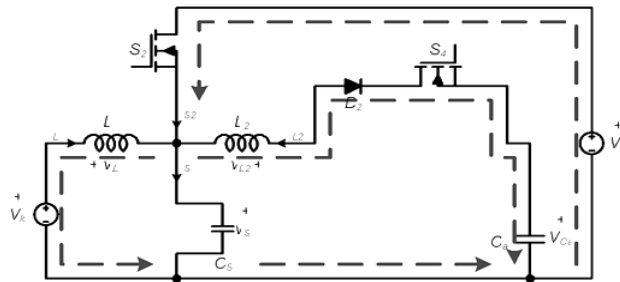
Mode5



Mode6



Mode7



Mode8

**Fig. 4(b):** Buck operation of the converter

At the end of this mode, the inductor currents  $i_{L1}$  and  $i_{L2}$  arrive at their maximum values  $-i_{m2}$  and  $i_{s1}$ , respectively. The currents  $-i_{m2}$  and  $i_{s1}$  can be obtained by

$$-i_{m2} = -I_{m1} + \frac{V_{Io}}{L_1} DT_S \quad (17)$$

$$I_{s1} = \frac{V_{Ca}}{L_2} \Delta T_S \quad (18)$$

Mode5[  $t_4, t_5$ ]:

The switch  $S_1$  is turned off at  $t_4$ . In a similar way to mode 5 in boost operation,  $v_{s1}$  and  $v_{s2}$  vary linearly. The transition time interval can be expressed as follows

$$T_{t2} = \frac{(C_{s1} + C_{s2})V_{hi}}{I_{s1} - I_{m2}} \quad (19)$$

Mode 6[  $t_5, t_6$ ]:

At  $t_5$ , the voltage  $V_{s1}$  arrives at  $V_{hi}$  and  $v_{s2}$  reaches zero with the turn-on of  $D_{s2}$ . In a similar way to mode 6 in boost operation, the ZVS of  $S_2$  is achieved. Since the voltages and across the each inductor are and respectively, the currents and decrease linearly as follows

$$i_{L1}(t) = -I_{m2} - \frac{V_{hi} - V_{Io}}{L_1} (t - t_5) \quad (20)$$

$$i_{L2}(t) = I_{s1} - \frac{V_{hi} - V_{Ca}}{L_2} (t - t_5) \quad (21)$$

The switch current  $i_{s2}$  is expressed as the sum of  $-i_{L1}$  from (20) and  $-i_{L2}$  from (21).

Mode 7 [ $t_6, t_7$ ]:

This mode begins when  $i_{L2}$  zero becomes and the blocking diode  $D_1$  is turned off. After that, the auxiliary switch  $S_3$  is turned off in the ZCS condition. The switch current  $i_{s2}$  is equal to the main inductor current  $-i_{L1}$  from (20).

Mode 8 [ $t_7, t_8$ ]:

At  $t_7$ , the auxiliary switch  $S_4$  is turned on. Since the voltage  $V_{L2}$  across the inductor  $L_2$  is  $-(V_{hi} - V_{Ca})$ , the inductor current  $i_{L2}$  decreases linearly with a slope of  $-(V_{hi} - V_{Ca})/L_2$  as follows

$$i_{L2}(t) = -\frac{V_{hi}-V_{Ca}}{L_2}(t - t_7) \tag{22}$$

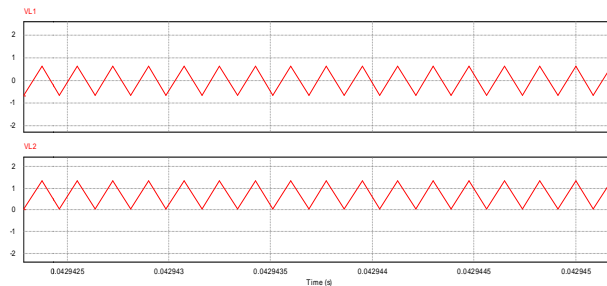
The switch current  $i_{s2}$  is the sum of  $-i_{L1}$  and  $-i_{L2}$  obtained from (20) and (22). At the end of this mode, the inductor currents  $i_{L1}$  and  $i_{L2}$  arrive at their minimum values  $-I_{m1}$  and  $-I_{s2}$  respectively. The currents  $-I_{m1}$  and  $-I_{s2}$  can be obtained by

$$-I_{m1} = -I_{m2} - \frac{V_{hi}-V_{Lo}}{L_1}(1 - D)T_S \tag{23}$$

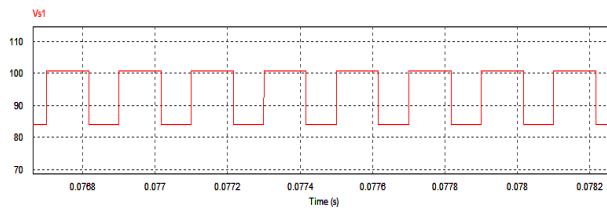
$$-I_{s2} = -\frac{V_{hi}-V_{Ca}}{L_2} \Delta T_S \tag{24}$$

**IV. Simulation Result:**

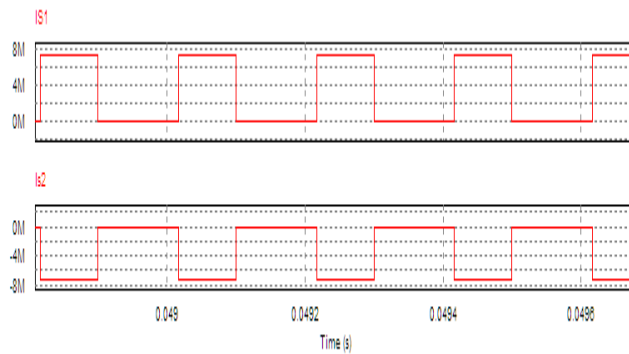
The system parameters are used given in the following waveforms.



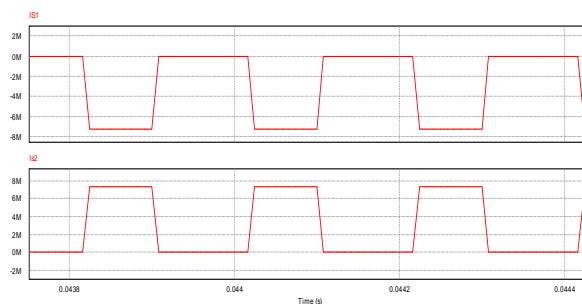
(a) Inductor voltage



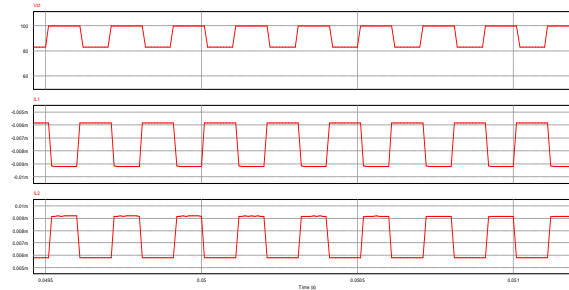
(b) Source voltage ( $V_{s1}$ )



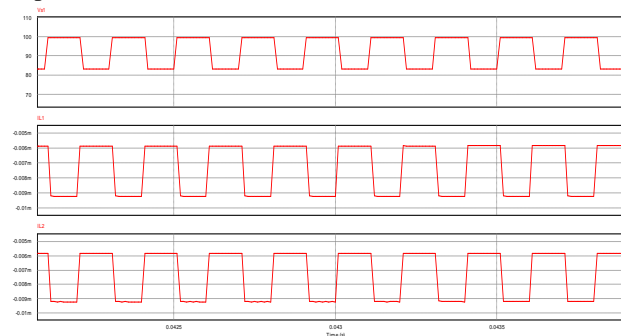
(c) Source current in boost mode operation



(c) Source current in buck mode operation



(d) Output waveform of boost operation



(e) Output waveform of buck operation

Since  $S_1$  acts as a synchronous switch in buck operation, ZVS of  $S_1$  is always satisfied. Therefore, ZVS of both  $S_1$  and  $S_2$  can be easily achieved by setting the time  $\Delta T_S$  at maximum power. The relationships between the inductance of the auxiliary inductor  $L_2$  and the time  $\Delta T_S$  that  $L_2$  is charging energy according to the output power  $P_o$  in boost and buck operations. In case of the conventional method, the efficiency  $\eta$  is considered as 3% more than the proposed method. In buck operation,  $\eta$  is not considered because the average current  $I_{I0}$  is equal to the output current  $I_o$ . Once the inductance of  $L_2$  is selected, the minimum time of  $\Delta T_S$  is obtained to achieve ZVS of main switches  $S_1$  and  $S_2$ .

#### Conclusion:

In this work, efficiency improvement in ZVS switched DC-DC converter has been proposed. In the proposed converter, ZVS of the main switches and ZCS of the auxiliary switches are always achieved. In addition, by utilizing the active snubber, there is no reverse-recovery problem of the intrinsic body diodes of the switches. Since the active snubber operates in a short time, the increased conduction loss of the proposed converter is relatively lower than the bidirectional dc-dc converter. Thus, the overall efficiency improvement is achieved over a wide range of load. Moreover, by adjusting according to loads, it is possible to achieve optimized overall efficiency throughout the whole loading range. At light load, the conduction loss can be reduced, and the efficiency can be improved by reducing  $\Delta T_S$ .

#### REFERENCES

- Hagbin, S., S. Lundmark, M. Alakula and O. Carlson, 2013. "Grid-connected integrated battery chargers in vehicle applications review and a new solution," *IEEE Trans. Ind. Electron.*, 60(2): 459-473.
- Cao, J. and A. Emadi, 2012. "A new battery/ultracapacitor hybrid Energy Storage system for electric, hybrid, and plug-in hybrid electric vehicles," *IEEE Trans. Ind. Electron.*, 27(1): 122-132.
- Park, T. and T. Kim, 2013. "Novel energy conversion system based on a multimode single-leg power converter," *IEEE Trans. Power Electron.*, 28(1): 213-220.
- Jang, M., M. Ciobotaru and V.G. Agelidis, 2013. "A single-phase grid-connected fuel cell system based on a boost-inverter," *IEEE Trans. Power Electron.*, 28(1): 279-288.
- Li, W., H. Wu, H. Yu, and X. He, 2011. "Isolated winding-coupled bidirectional ZVS converter with PWM plus phase-shift (PPS) control strategy," *IEEE Trans. Power Electron.*, 26(12): 3560-3570.
- Rolak, M. and M. Malinowski, 2011. "Dual active bridge for energy storage system in small wind turbine," in *Proc. AFRICON*, pp: 1-5.
- Jayasinghe, S.D.G., D.M. Vilathgamuwa and U.K. Madawala, 2011. "Diode-clamped three-level inverter-based battery/super-capacitor direct integration scheme for renewable energy systems," *IEEE Trans. Power Electron.*, 26(12): 3720-3729.

Arias, M., M.M. Hernando, D.G. Lamar, J. Sebastián and A. Fernández, 2012. "Elimination of the transfertime effects in line-interactive and passive standby UPSs by means of a small-size inverter," *IEEE Trans. Ind. Electron*, 27(3): 1468 -1478.

Yao, C., X. Ruan, X.Wang and C.K. Tse, 2011. "Isolated buck-boost DC/DC converters suitable for wide input-voltage range," *IEEE Trans. Power Electron*, 26(9): 2599-2613.

Lee, J.-Y., Y.-S. Jeong and B.-M. Han, 2011. "An isolated DC/DC converter using high-frequency unregulated resonant converter for fuel cell applications," *IEEE Trans. Ind. Electron.*, 58(7): 2926-2934.

Vinnikov, D. and I. Roasto, 2011. "Quasi-Z-source-based isolated DC/DC converters for distributed power generation," *IEEE Trans. Ind. Electron*, 58(1): 192-201.

Wu, T.-F., Y.-C. Chen, J.-G. Yang and C.-L. Kuo, 2010. "Isolated bidirectional full-bridge DC-DC converter with a flybacksnubber," *IEEE Trans. Power Electron*, 25(7): 1915-1922.

Singh, R.K. and S. Mishra, 2013. "Amagnetically coupled feedback-clamped optimal bi-directional battery charger," *IEEE Trans. Ind. Electron.*, 60(2): 422-432.

Wu, H., J. Lu, W. Shi and Y. Xing, 2012. "Nonisolated bidirectional DC-DC converters with negative-coupled inductor," *IEEE Trans. Power Electron*, 27(5): 2231-2235.

Das, P., S.A. Mousavi and G. Moschopoulos, 2010. "Analysis and design of a nonisolated bidirectional ZVS-PWM DC-DC converter with coupled inductors," *IEEE Trans. Power Electron.*, 25(10): 2630-2641.

Das, P., B. Laan, S.A. Mousavi and G. Moschopoulos, 2009. "A nonisolated bidirectional ZVS-PWM active clamped DC-DC converter," *IEEE Trans. Power Electron*, 24(2): 553-558.

Do, H.-L., 2011. "Nonisolated bidirectional zero-voltage-switching DC-DC converter," *IEEE Trans. Power Electron*, 26(9): 2563-2569.

Jung, D.-Y., S.-H.Hwang, Y.-H. Ji, J.-H. Lee, Y.-C. Jung, and C.-Y. Won, 2013. "Soft-switching bidirectional DC/DC converter with an LC series resonant circuit," *IEEE Trans. Power Electron.*, 28(4) 1680-1690.

Lin, B.-R. and C.-H.Chao, 2013. "Analysis, design, and implementation of a soft-switching converter with two three-level PWM circuits," *IEEE Trans. Power Electron*, 28(4): 1700-1710.